



AUSTRALIAN ATOMIC ENERGY COMMISSION
RESEARCH ESTABLISHMENT
LUCAS HEIGHTS

keV NEUTRON CAPTURE IN ZIRCONIUM-91

by

J. W. BOLDEMAN

B. J. ALLEN

A. R. deL MUSGROVE

*R. L. MACKLIN

* Oak Ridge National Laboratory, Oak Ridge, Tennessee, USA.
Research sponsored in part by the USAEC under contract to Union
Carbide Corporation.

January 1976

ISBN 0 642 99279 2

AUSTRALIAN ATOMIC ENERGY COMMISSION
RESEARCH ESTABLISHMENT
LUCAS HEIGHTS

keV NEUTRON CAPTURE IN ZIRCONIUM-91

by

J.W. BOLDEMAN
B.J. ALLEN
A.R. deL MUSGROVE
*R.L. MACKLIN

ABSTRACT

The neutron capture cross section of ^{91}Zr has been measured with high resolution ($\Delta E/E \sim 0.2$ per cent) between 3 and 30 keV. Values of the $g\Gamma_n\Gamma_\gamma/\Gamma$ for 119 resonances in this energy range have been obtained. The average capture cross section is consistent with values of $\langle\Gamma_{ys}\rangle = \langle\Gamma_{yp}\rangle = 200$.

* Oak Ridge National Laboratory, Oak Ridge, Tennessee, USA.
Research sponsored in part by the USAEC under contract to Union Carbide Corporation.

National Library of Australia card number and ISBN 0 642 99279 2

The following descriptors have been selected from the INIS Thesaurus to describe the subject content of this report for information retrieval purposes. For further details please refer to IAEA-INIS-12 (INIS: Manual for Indexing) and IAEA-INIS-13 (INIS: Thesaurus) published in Vienna by the International Atomic Energy Agency.

CAPTURE; CROSS SECTIONS; ENERGY DEPENDENCE; KEV RANGE 10-100; NEUTRON REACTIONS; RESONANCE; ZIRCONIUM 91 TARGET

CONTENTS

	Page
1. INTRODUCTION	1
2. EXPERIMENTAL METHOD AND DATA ANALYSIS	1
3. RESULTS	2
4. REFERENCES	2

Table 1 Resonance Parameters for ^{91}Zr

- Figure 1 Uncorrected experimental capture yield
- Figure 2 Plot of capture kernel versus neutron energy
- Figure 3 Staircase plot of number of resonances below energy E
- Figure 4 Comparison of experimental data with statistical model calculations of capture cross section assuming $S_0 = 0.5 \times 10^{-4}$, $S_1 = 5 \times 10^{-4}$, $\Gamma_{\gamma s} = \Gamma_{\gamma p} = 0.2 \text{ eV}$ and $\langle D_s \rangle = 660 \text{ eV}$

1. INTRODUCTION

The neutron capture cross section of ^{91}Zr has been measured between 3 and 30 keV using the neutron capture facility at the 40 m flight path of the Oak Ridge Electron Linear Accelerator (ORELA). In previous studies of $^{90,92,94}\text{Zr}$ [Boldeman et al. 1975a,b], strong non-statistical effects were observed in the neutron capture cross section which were attributed to single-particle effects associated with the $N=50$ closed shell and the peak in the p-wave strength function at $A \sim 95$. The non-statistical effect, consisting of significant correlations between the reduced neutron and radiative width for p-wave resonances, found a satisfactory quantitative explanation in terms of the optical model formulation of the valence theory and a doorway state mechanism. In contrast, for neutron capture in odd A ^{91}Zr these effects will be between one and two orders of magnitude less, largely because of smaller reduced neutron widths, and the capture cross section of ^{91}Zr should behave in a statistical manner.

From the data viewpoint, information on ^{91}Zr is of value because of the use of Zr in reactor systems and the occurrence of ^{91}Zr as an important fission product (WRENDA Requests Nos. 691156, 691155).

2. EXPERIMENTAL METHOD AND DATA ANALYSIS

The experimental system has been described in considerable detail [Boldeman et al. 1975a, Macklin & Allen 1971]. The neutron capture gamma-ray detector consisted of two non-hydrogenous liquid scintillators with low neutron sensitivity which operated under a pulse height weighting scheme such that the efficiency of the device is a function only of the total gamma-ray energy release. The neutron monitor was a thin ^6Li glass scintillator (0.5 mm thick) located 1 metre upstream of the capture detector and therefore operated in the transmission mode. The relative neutron detection efficiency of the ^6Li monitor was based on an evaluation of the $^6\text{Li}(n,\alpha)$ cross section which included the evaluation of Uttley et al. [1971] below 100 keV and recent experimental data from Fort & Marquette [1972], Coates et al. [1972] and Poenitz [1974] above that energy. The capture detector efficiency was deduced using the ^6Li glass detector and observing the saturated capture yield from the 4.9 eV resonance in Au. An enriched target (88.5 per cent ^{91}Zr) was used. Resonances in the other Zr isotopes were removed using the data from Boldeman et al. [1975a,b].

The method of analysis has been described in detail by Musgrove et al. [1974] and is based on the ORNL/RPI code of Sullivan et al. [1969]. The Monte Carlo code uses initial guesses for the resonance neutron (Γ_n) and

radiative widths (Γ_γ) to determine self-shielding and multiple-scattering corrections. An iterative fit is then made to the capture area for each resonance ($2\pi^2\chi^2 g\Gamma_n\Gamma_\gamma/\Gamma$) by varying whichever of the initial values of Γ_γ and Γ_n is the smaller. The analysis of the capture cross section data for ^{91}Zr was somewhat restricted by the absence of a suitable total cross section measurement and therefore by the lack of values of Γ_n for the resonances studied. For several resonances in the present data set, shape analysis of the capture data leading to a value of Γ_n was possible. These values of Γ_n have been used in the analytical procedure. Otherwise it has been assumed that $\Gamma_n > \Gamma_\gamma$ for all resonances and a value of Γ_n equal to one fifth of the resolution width ($\Gamma_R \approx 0.2$ per cent) has been used. The broad resonance at 3.991 keV listed by Mughabghab & Garber [1973] was found to have $\Gamma_n \leq 3$ eV in the present data. The absence of any spin data whatsoever for the resonances studied restricts the resonance analysis to the production of the capture kernel only ($g\Gamma_n\Gamma_\gamma/\Gamma$).

3. RESULTS

Figure 1 shows the capture yield data for the energy region between 3 and 30 keV, while Table 1 lists the output data for the 120 resonances identified in this region. Figure 2 is a staircase plot of the observed levels below 30 keV; this shows that few levels have been missed to 30 keV. If the level density is independent of parity and shows a $(2J+1)$ dependence, an s-wave level spacing of 670 eV is obtained.

Figure 3 is a plot of the capture kernel versus neutron energy. There is no feature of the plot which allows any distinction to be made between s- or p-wave resonances or, for that matter, between the allowed values of g . The most interesting feature of Figure 3 is the absence of large values of the capture kernel and the narrow distribution of the measured values. This behaviour contrasts quite strongly with equivalent data for $^{90,92,94}\text{Zr}$, where the variance of the capture kernels was significantly greater than the mean. This feature of the data is entirely expected for ^{91}Zr as non-statistical effects are estimated to be between one and two orders of magnitude less than for $^{90,92,94}\text{Zr}$. The major reason for the large reduction in non-statistical effects arises because of the reduced neutron widths of the resonances, which are approximately a factor of 40 less than for ^{90}Zr .

The average capture cross section is shown for ^{91}Zr in Figure 4. Also shown is the calculated statistical model capture cross section obtained using the published values of Mughabghab & Garber [1973] for

the strength function, the present value of 670 eV for the s-wave level spacing, and assuming an average radiative width of 200 meV for both s-wave and p-wave resonances. The calculated cross section is in agreement with the experimental values. The 30 keV cross section from the present experiment, *i.e.* 60 ± 6 mb, is in close agreement with the two previous measurements, 60 ± 6 mb from Kapchigashev [1964] and 59 ± 10 from Macklin *et al.* [1963].

4. REFERENCES

1. Boldeman, J.W., Allen, B.J., Musgrove, A.R. deL. & Macklin, R.L. [1975a] Nucl. Phys., A246:1.
2. Boldeman, J.W., Allen, B.J., Musgrove, A.R. deL., Kenny, M.J. & Macklin, R.L. [1975b] Valence and Doorway State Effects in Neutron Capture near Closed Shells. Paper presented to the 3rd National Soviet Conference on Neutron Physics, Kiev.
3. Macklin, R.L. & Allen, B.J. [1971] Nucl. Instrum. Methods, 91:565.
4. Uttley, C.A., Sowerby, M.G., Patrick, B.H. & Rae, E.R. [1971] CONF-710301, Vol. I:551.
5. Fort, E. & Marquette, J.P. [1972] Proc. 2nd IAEA Panel on Neutron Standard Reference Data, November 1972 Vienna. IAEA, Vienna, p.113.
6. Coates, M.S., Hunt, G.J. & Uttley, C.A. [1972] Proc. 2nd IAEA Panel on Neutron Standard Reference Data, November 1972 Vienna. IAEA, Vienna, p.110.
7. Poenitz, W.P., [1974] Z., Phys., 268:359.
8. Musgrove, A.R. deL., Allen, B.J. & Macklin, R.L. [1974] AAEC/E327.
9. Sullivan, J.G., Warner, G.C., Block, R.C. & Hockenbury, R.W. [1969] Rensselaer Polytechnic Institute-USAEC Report RPI-328-155 (unpublished).
10. Mughabghab, S.F. & Garber, D.I. [1973] - BNL-325, 3rd ed.
11. Kapchigashev, S.P. [1964] At. Ehnerg., 19:294.
12. Macklin, R.L., Gibbons, J.H. & Inada, I. [1963] Nucl. Phys., 43:353.

TABLE 1
 RESONANCE PARAMETERS FOR ^{91}Zr

Energy (keV)	Γ_n (eV)	$g\Gamma_n\Gamma_\gamma/\Gamma$ (eV)	Energy (keV)	Γ_n (eV)	$g\Gamma_n\Gamma_\gamma/\Gamma$ (eV)
3.162±0.006	(1.4) ^a	0.085±0.009	8.510±0.017		0.073±0.008
3.617±0.007		0.052±0.005	8.527±0.017		0.066±0.007
3.648±0.007		0.054±0.005	8.865±0.018	15±5	0.014±0.002
3.869±0.008		0.064±0.006	8.955±0.018		0.046±0.005
4.012±0.008	<3	0.064±0.006	9.045±0.018		0.071±0.007
4.283±0.008		0.052±0.005	9.109±0.018		0.069±0.007
4.333±0.009	5±2	0.214±0.021	9.239±0.018	5 ⁺³ ₋₂	0.075±0.008
4.754±0.010		0.082±0.008	9.310±0.019		0.037±0.006
4.985±0.010		0.045±0.005	9.839±0.020		0.115±0.012
5.367±0.011		0.012±0.002	9.885±0.020	10±4	0.052±0.006
5.533±0.011	15±5	0.062±0.006	10.001±0.020		0.106±0.011
5.640±0.011		0.069±0.007	10.14 ±0.02		0.106±0.011
5.832±0.012		0.058±0.006	10.53 ±0.02		0.084±0.009
6.098±0.012		0.029±0.003	10.56 ±0.02		0.078±0.008
6.187±0.012		0.006±0.002	10.71 ±0.02		0.085±0.009
6.481±0.013		0.060±0.006	10.75 ±0.02		0.065±0.007
6.768±0.014		0.044±0.005	11.08 ±0.02		0.078±0.008
6.867±0.014		0.050±0.005	11.11 ±0.02		0.016±0.003
7.047±0.014	5±3	0.151±0.015	11.13 ±0.02		0.048±0.005
7.134±0.014		0.089±0.009	11.24 ±0.02		0.063±0.007
7.267±0.015	4 ⁺⁴ ₋₁	0.095±0.010	12.12 ±0.02		0.088±0.009
7.362±0.015		0.064±0.006	12.18 ±0.02		0.017±0.004
7.768±0.015	5 ⁺³ ₋₂	0.203±0.020	12.23 ±0.02		0.147±0.015

TABLE 1 (cont'd)

Energy (keV)	Γ_n (eV)	$g\Gamma_n\Gamma_\gamma/\Gamma$ (eV)	Energy (keV)	Γ_n (eV)	$g\Gamma_n\Gamma_\gamma/\Gamma$ (eV)
12.33±0.02		0.056±0.006	18.56±0.04		0.050±0.007
12.56±0.03		0.143±0.014	18.66±0.04		0.155±0.016
12.94±0.03		0.059±0.006	19.52±0.04		0.159±0.016
13.17±0.03		0.077±0.008	19.61±0.04		0.069±0.008
13.27±0.03		0.078±0.008	19.78±0.04		0.086±0.010
13.32±0.03		0.083±0.009	19.83±0.04		0.074±0.009
13.58±0.03		0.048±0.006	20.04±0.04		0.060±0.009
13.71±0.03		0.141±0.014	20.19±0.04		0.144±0.015
13.81±0.03		0.058±0.006	20.20±0.04	20±10	0.168±0.017
14.10±0.03		0.077±0.008	20.27±0.04		0.069±0.009
14.20±0.03		0.050±0.006	20.32±0.04		0.056±0.808
14.26±0.03		0.083±0.009	20.41±0.04		0.071±0.009
14.60±0.03		0.111±0.012	20.65±0.04		0.089±0.010
14.86±0.03		0.071±0.008	20.92±0.04		0.127±0.013
15.19±0.03		0.165±0.017	21.25±0.04		0.075±0.009
15.25±0.03		0.068±0.007	21.32±0.04		0.064±0.009
15.78±0.003		0.064±0.007	21.52±0.04		0.081±0.010
16.20±0.03		0.075±0.008	21.72±0.04	100±30	0.048±0.007
16.71±0.03		0.069±0.008	21.78±0.04		0.106±0.011
16.86±0.03		0.034±0.005	22.19±0.04		0.077±0.009
16.99±0.03		0.070±0.008	22.48±0.04		0.081±0.010
17.07±0.03		0.050±0.007	22.62±0.05		0.062±0.008
17.47±0.03		0.103±0.011	22.76±0.05		0.073±0.009
17.82±0.04		0.132±0.014	22.82±0.05		0.127±0.013

TABLE 1 (cont'd)

Energy (keV)	Γ_n (eV)	$g\Gamma_n\Gamma_\gamma/\Gamma$ (eV)	Energy (keV)	Γ_n (eV)	$g\Gamma_n\Gamma_\gamma/\Gamma$ (eV)
23.34±0.05		0.088±0.010	27.13±0.05		0.196±0.021
23.72±0.05		0.101±0.011	27.39±0.05		0.072±0.010
24.24±0.05	40±15	0.364±0.037	27.61±0.06		0.130±0.014
24.33±0.05		0.077±0.010	27.95±0.06		0.110±0.012
24.81±0.05		0.089±0.011	28.06±0.06		0.131±0.014
24.93±0.05		0.141±0.015	28.77±0.06		0.088±0.010
25.28±0.05		0.093±0.011	28.96±0.06		0.183±0.019
25.72±0.05		0.080±0.010	29.09±0.06		0.148±0.015
26.00±0.05		0.207±0.021	29.18±0.06		0.106±0.011
26.58±0.05		0.102±0.012	29.34±0.06		0.064±0.008
26.95±0.05		0.051±0.007	29.55±0.06		0.143±0.015
27.30±0.05		0.105±0.012	29.74±0.06		0.134±0.014
			30.06±0.06		0.194±0.020

()^a Γ_n value assumed

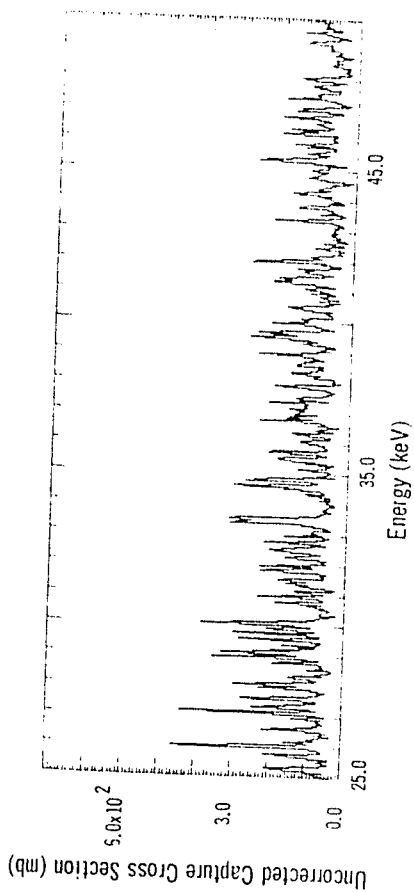
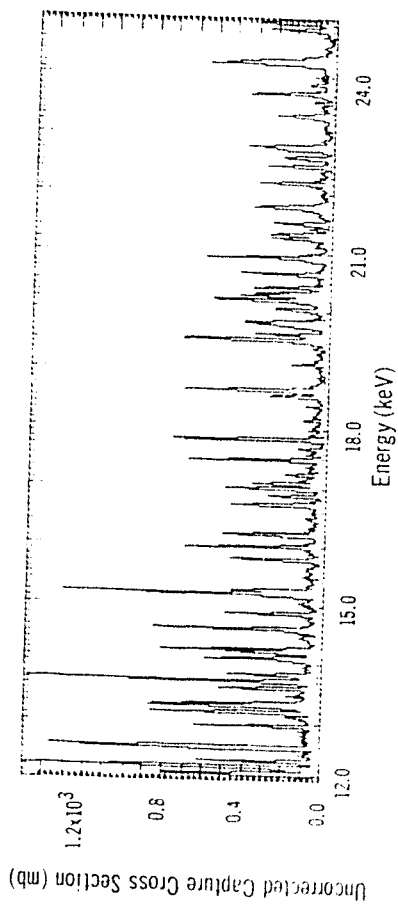
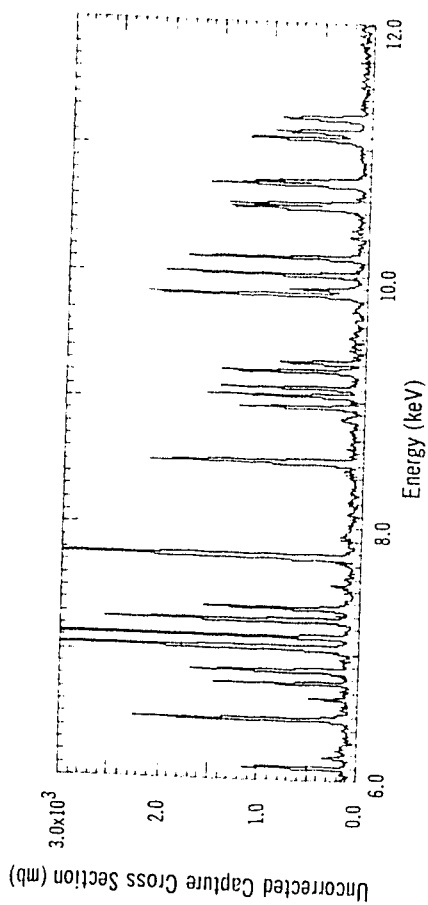
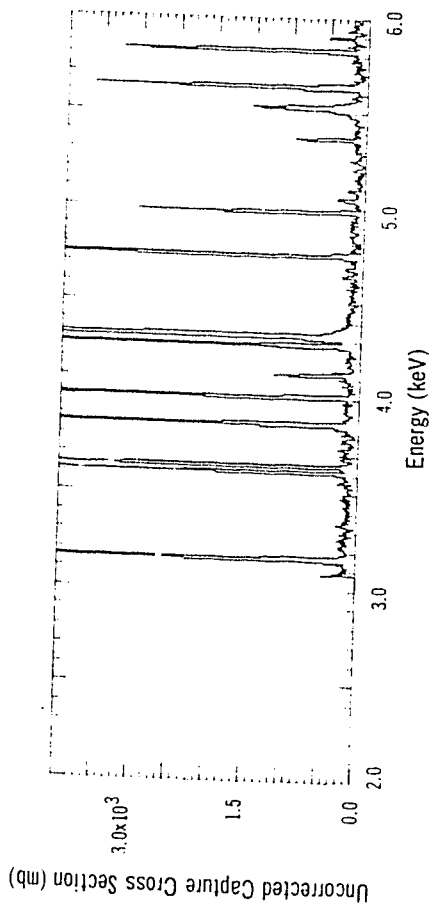


FIGURE 1. UNCORRECTED EXPERIMENTAL CAPTURE YIELD

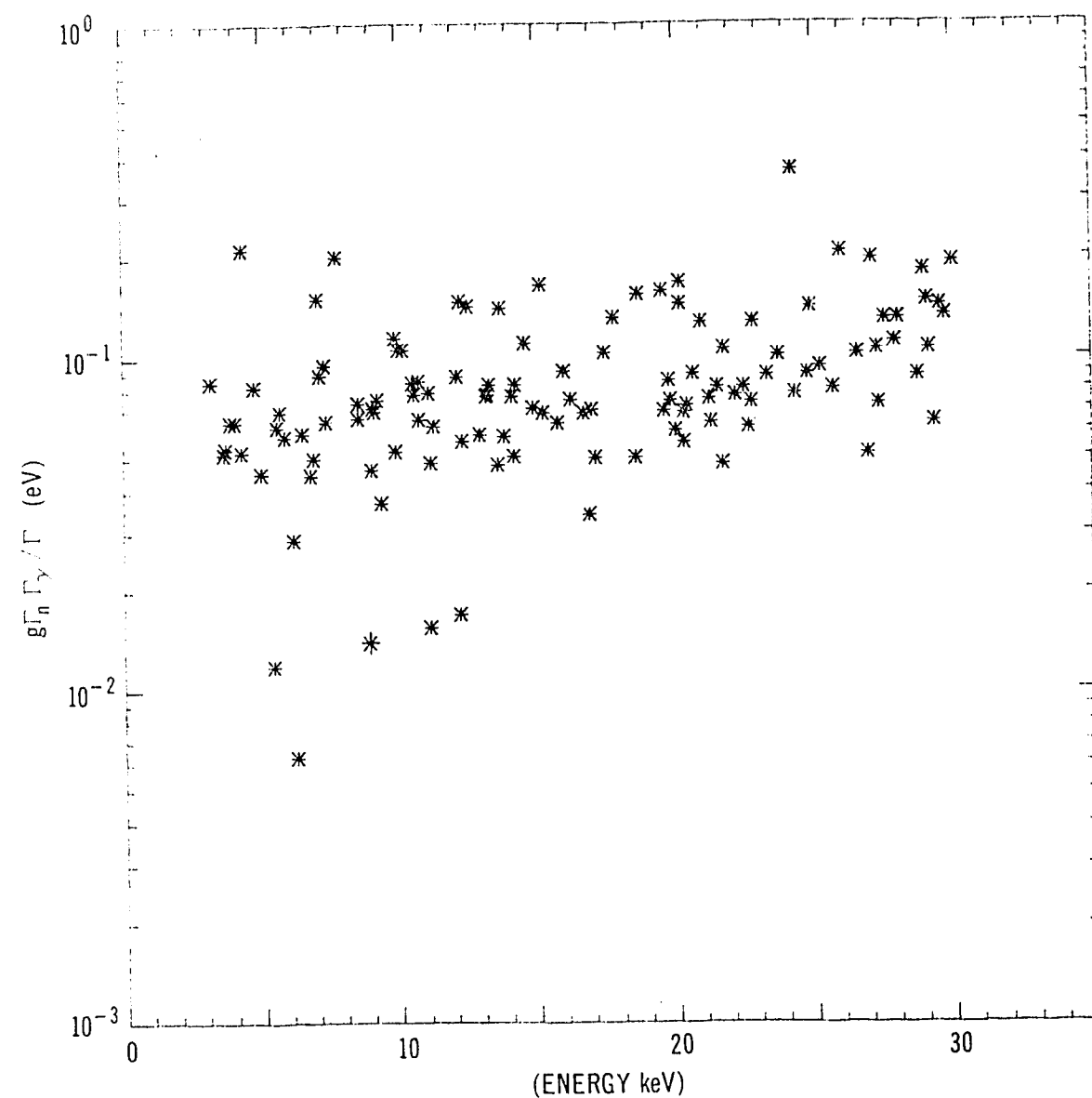


FIGURE 2. PLOT OF CAPTURE KERNEL VERSUS NEUTRON ENERGY

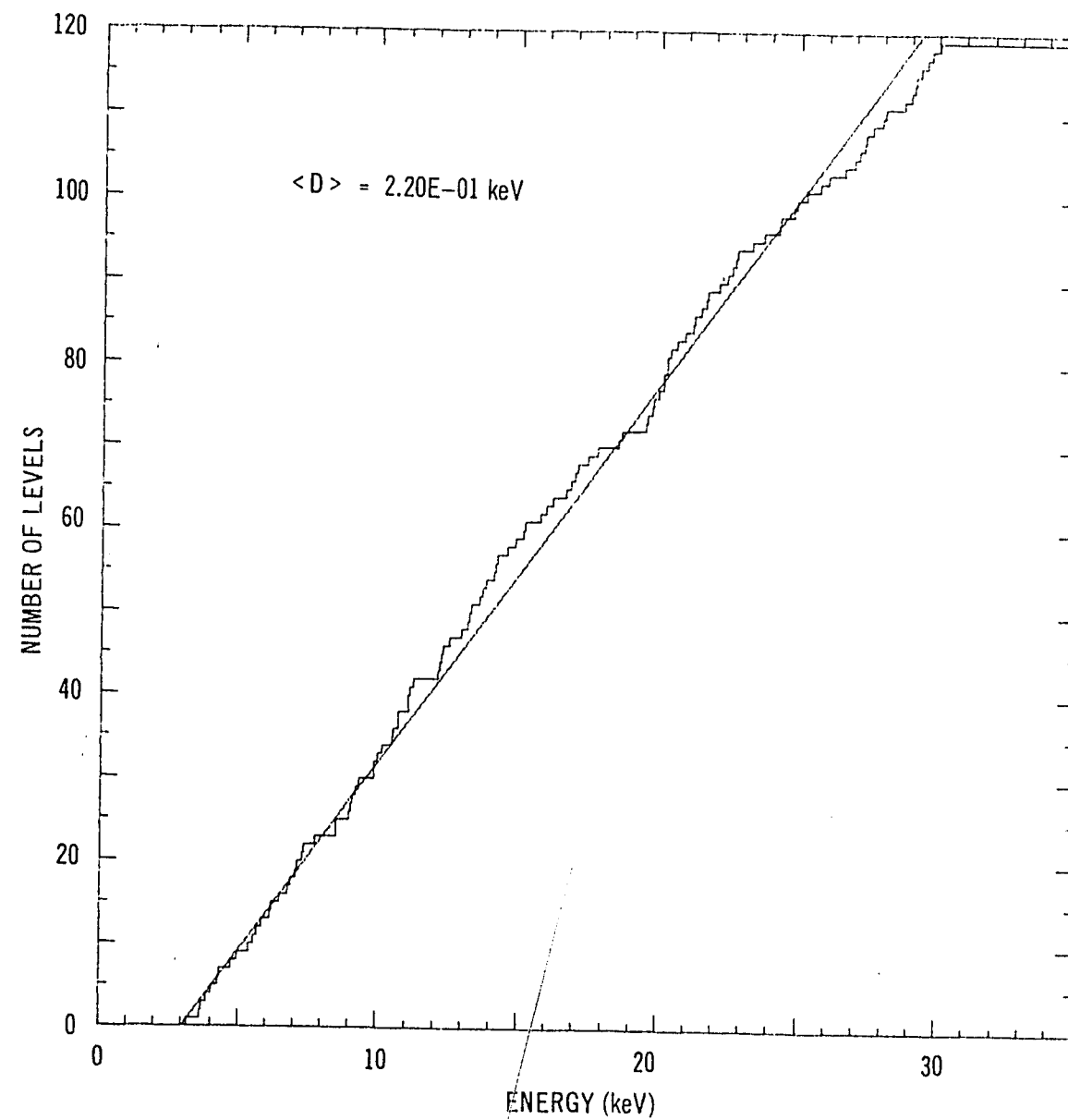


FIGURE 3. STAIRCASE PLOT OF NUMBER OF RESONANCES BELOW ENERGY E

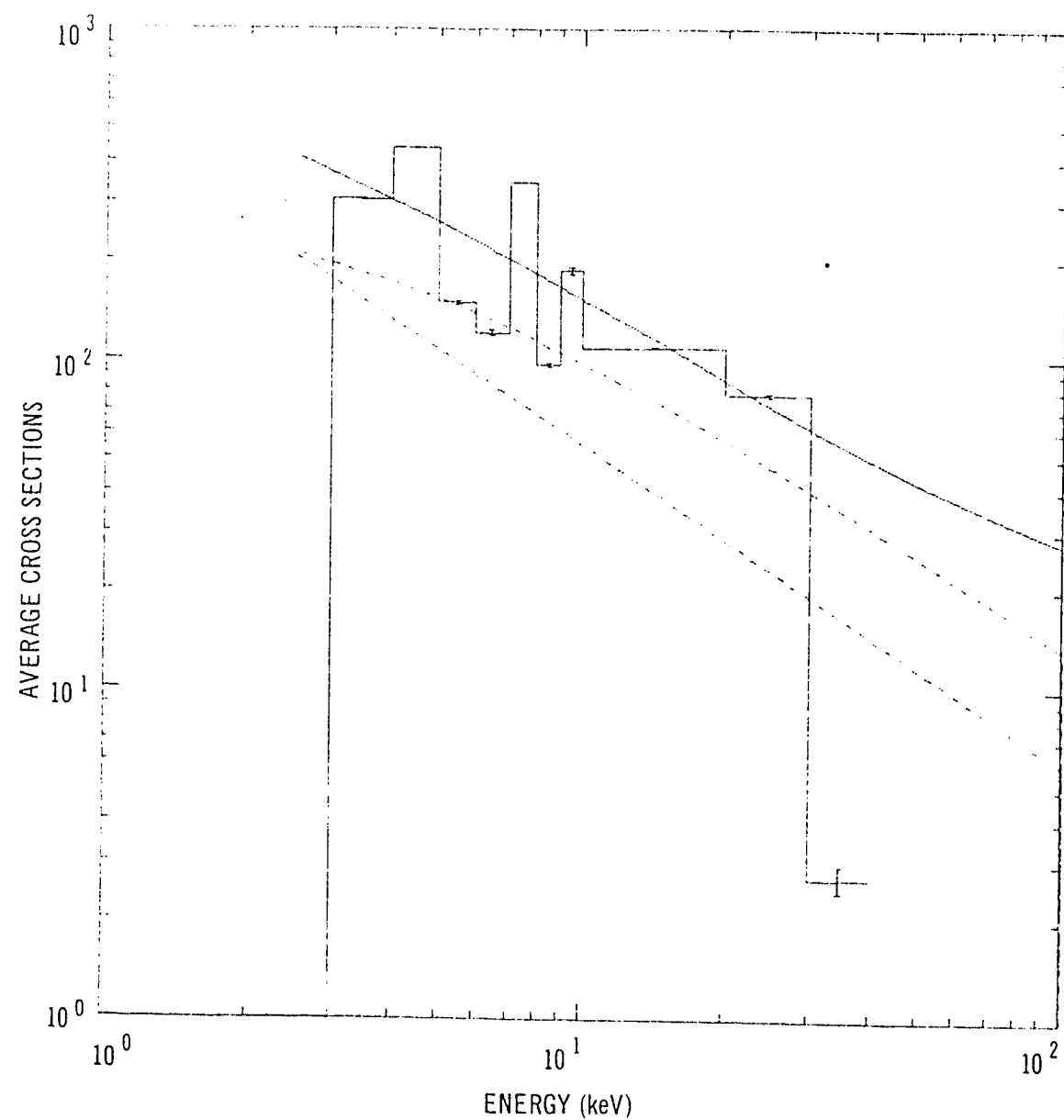


FIGURE 4. COMPARISON OF EXPERIMENTAL DATA WITH STATISTICAL
MODEL CALCULATIONS OF CAPTURE CROSS SECTION
ASSUMING $S_0 = 0.5 \times 10^{-4}$, $S_1 = 5 \times 10^{-4}$,
 $\Gamma_{\gamma s} = \Gamma_{\gamma p} = 0.2 \text{ eV}$ AND $\langle D_s \rangle = 660 \text{ eV}$

